

TPP: Test-Time Padding for Adversarial Detection and Robust Adaptation on Vision-Language Models

Zhiwei Li^{1,2*} Yitian Pang^{3*} Weining Wang² Zhenan Sun^{1,2} Qi Li^{1,2}

¹NLPR & MAIS, Institute of Automation, Chinese Academy of Sciences

²University of Chinese Academy of Sciences

³School of Automation, Tsinghua University

lizhiwei2023@ia.ac.cn, pangyt23@mails.tsinghua.edu.cn, {weining.wang, znsun, qli}@nlpr.ia.ac.cn

Abstract

Vision-Language Models (VLMs), such as CLIP, have achieved impressive zero-shot recognition performance but remain highly susceptible to adversarial perturbations, posing significant risks in safety-critical scenarios. Previous training-time defenses rely on adversarial fine-tuning, which requires labeled data and costly retraining, while existing test-time strategies fail to reliably distinguish between clean and adversarial inputs, thereby preventing both adversarial robustness and clean accuracy from reaching their optimum. To address these limitations, we propose Test-Time Padding (TPP), a lightweight defense framework that performs adversarial detection followed by targeted adaptation at inference. TPP identifies adversarial inputs via the cosine similarity shift between CLIP feature embeddings computed before and after spatial padding, yielding a universal threshold for reliable detection across architectures and datasets. For detected adversarial cases, TPP employs trainable padding to restore disrupted attention patterns, coupled with a similarity-aware ensemble strategy for a more robust final prediction. For clean inputs, TPP leaves them unchanged by default or optionally integrates existing test-time adaptation techniques for further accuracy gains. Comprehensive experiments on diverse CLIP backbones and fine-grained benchmarks show that TPP consistently surpasses state-of-the-art test-time defenses, delivering substantial improvements in adversarial robustness without compromising clean accuracy. The code for this paper will be released soon.

1. Introduction

Vision-Language Models (VLMs) [3, 31, 52], pretrained on large-scale image–text pairs, have achieved remarkable zero-shot generalization across a wide range of downstream

*Equal contribution.

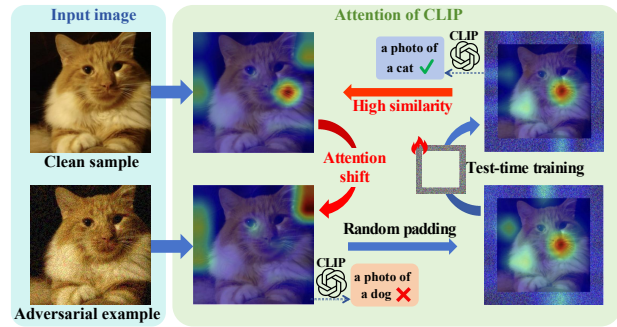


Figure 1. Visualization of attention maps for clean sample, adversarially perturbed sample, randomly padded sample, and samples processed with trainable test-time padding. The adversarial attack causes a noticeable shift in attention, leading to incorrect predictions. Applying random padding helps restore the original attention focus, while trainable padding further refines the attention to the correct regions and suppresses noise, resulting in more accurate predictions.

tasks. Among them, CLIP [31] has emerged as a milestone model that aligns visual and textual representations through contrastive learning, enabling powerful cross-modal understanding. Owing to its transparent architecture and strong transferability, CLIP has become a cornerstone of modern multimodal research, driving progress in computer vision [14, 31], medical imaging [13, 45], and robotics [1, 34]. Despite its impressive generalization, CLIP is notably fragile under adversarial perturbations, which can severely degrade performance [5, 16, 26, 38, 54]. Retraining such large-scale models from scratch is computationally prohibitive, leading most users to rely on public pretrained checkpoints and further amplifying the risks posed by adversarial attacks.

To improve robustness, prior studies have explored adversarial prompt tuning (APT) [19, 43, 55], which learns robust text prompts via adversarial training. However, these

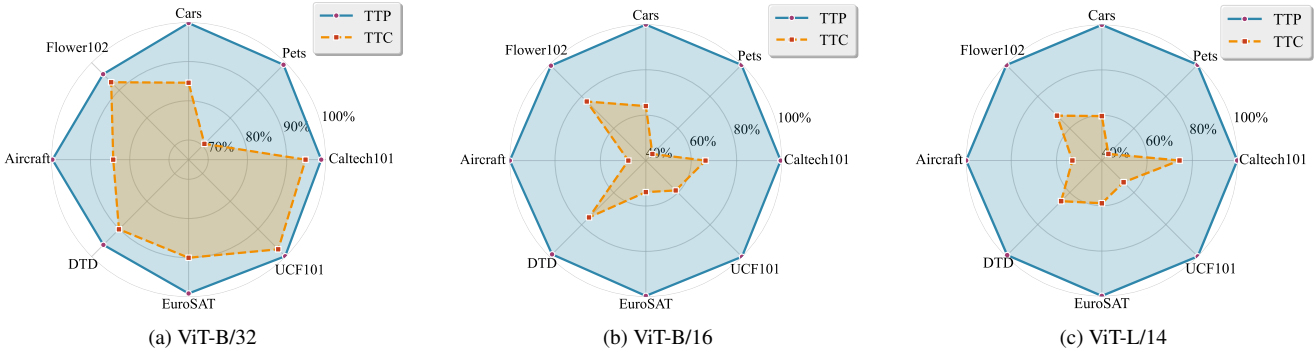


Figure 2. Detection accuracy of TTP (ours) and TTC [47] across fine-grained classification datasets under three CLIP backbones (ViT-B/32, ViT-B/16, and ViT-L/14). All experiments are performed under the same attack strength of $\epsilon = 4.0$. TTC adopts its default L_2 -distance threshold $\tau = 0.2$, but exhibits pronounced fluctuations in detection performance across both datasets and backbones, indicating its sensitivity to domain and model variations. In contrast, our TTP employs a unified cosine similarity threshold $\tau = 0.8$, yet maintains consistently superior detection accuracy across all settings. This demonstrates that TTP achieves not only outstanding adversarial recognition capability but also remarkable cross-dataset and cross-backbone stability, effectively mitigating the instability observed in TTC under identical conditions.

methods require labeled adversarial data and costly retraining, and their robustness fails to generalize beyond seen categories. In contrast, test-time defense methods [33, 40, 44] adapt models on the fly but typically apply uniform adaptation to all inputs, leading to suboptimal performance on both robustness and clean accuracy. The recent Test-Time Counterattack (TTC) [47] reports that adversarial examples exhibit greater stability under small perturbations, enabling discrimination between clean and adversarial inputs by measuring feature stability under slight noise. However, TTC exhibits low detection accuracy and poor generalization across datasets and model architectures (Figure 2), which severely constrains its practical utility in unseen scenarios.

To address these limitations, we propose Test-Time Padding (TTP), a simple yet highly effective framework for robust inference with CLIP. Our key insight is that image padding can restore attention disrupted by adversarial perturbations (as shown in Figure 1), producing distinct similarity shifts between clean and adversarial examples. Specifically, by comparing visual embeddings before and after padding, we observe that clean samples exhibit minimal feature change, whereas adversarial examples show significant shifts. This observation enables a unified, dataset-agnostic criterion for reliable adversarial detection. As shown in Figure 2, compared to TTC, our proposed method achieves uniformly superior performance across diverse datasets and model architectures using a single, unified cosine-similarity threshold.

Based on accurate detection, TTP dynamically differentiates inference strategies for clean and adversarial inputs. Clean samples are directly preserved to maintain semantic integrity and clean accuracy. For adversarial exam-

ples, our prior findings have shown that random padding can effectively recover attention patterns disrupted by adversarial perturbations. To further improve defense performance, we introduce trainable test-time padding. During inference, multiple augmented views of each adversarial instance are generated, and padding parameters are optimized by a single step via entropy minimization over high-confidence samples. To achieve a more robust final prediction, we introduce a similarity-aware ensemble that assigns adaptive weights to each augmented view by measuring its similarity to the adversarial example’s embeddings before and after padding, thereby further strengthening the defense performance. In summary, our main contributions are as follows:

- We show that spatial padding restores attention patterns disrupted by adversarial perturbations and use similarity shift to build a unified detector that generalizes across datasets and architectures.
- For detected adversarial inputs, we introduce single-step trainable padding at inference and a similarity-aware ensemble, yielding more reliable predictions.
- Combining detection with robust adaptation, we propose TTP, a two-stage detect-then-adapt defense that consistently improves robustness without sacrificing clean accuracy across multiple CLIP backbones and fine-grained datasets, significantly surpassing prior test-time defenses.

2. Related Work

2.1. Adversarial Attacks and Defenses

Adversarial attacks expose the vulnerability of neural networks by introducing imperceptible perturbations that mislead predictions [9, 24, 39]. Gradient-based white-box at-

tacks, such as FGSM [9] and BIM [18], generate adversarial examples through iterative or single-step gradient updates [23, 51, 56]. Among them, PGD (Projected Gradient Descent) [24] has become the *de facto* standard benchmark for evaluating model robustness due to its strong attack capability and generality. In contrast, black-box attacks, including transfer-based [21] and query-based variants [6, 10, 42, 51, 53], operate without gradient access, reflecting more realistic threat scenarios. These attack families collectively demonstrate the fragility of high-level representations even in large-scale pretrained VLMs such as CLIP, motivating the study of efficient and model-agnostic defenses.

Existing defenses focus primarily on improving the stability of the model against perturbations [20, 24, 46, 50]. Adversarial training and its variants remain the most effective but require extensive labeled data and retraining. For vision-language models, robust fine-tuning strategies such as TeCoA [26] and APT [19], which adjust prompts or image encoders through adversarially augmented data, achieving improved robustness but at high computational and data costs. Our work follows an alternative direction—**test-time robust adaptation**, which optimizes model behavior on-the-fly without modifying pretrained weights.

2.2. Test-Time Adaptation and Defense for VLMs

Test-time adaptation (TTA) has emerged as an effective strategy to improve generalization on unseen domains during inference [15, 22, 27, 37, 48]. Representative approaches such as TENT [41], TPT [35], and DiffTPT [8] adapt model parameters or prompts by minimizing prediction entropy across augmented test views. Ensemble-based methods [32, 49] further enhance stability by aggregating multiple views or prompt variants. These methods effectively mitigate distribution shifts and improve zero-shot accuracy but overlook robustness concerns, as they assume clean input data and stationary test distributions.

Recent studies extend TTA to adversarial scenarios, with the aim of improving the robustness of the model without retraining. TAPT [44] optimizes both textual and visual prompts by minimizing a marginal entropy objective, while R-TPT [33] takes a different route, decomposing the entropy objective into a pointwise loss to adapt only the text prompt during inference. Although both approaches achieve notable robustness gains, they share a fundamental flaw: they apply a uniform adaptation strategy to all inputs. This design is inherently suboptimal, as the conflicting adaptation objectives for clean and adversarial inputs limit the overall performance.

TTC [47] employs a different two-stage paradigm. It first distinguishes between inputs by measuring their feature embedding shifts under small perturbations, enabling separate optimization. However, its detection mechanism

suffers from poor accuracy and limited generalization. In contrast, our Test-Time Padding (TTP) improves this two-stage approach. By enabling highly accurate and generalizable adversarial detection, it applies a dedicated adaptation mechanism only where needed, substantially enhancing robustness without compromising the integrity of clean data.

3. Methodology

3.1. Preliminaries

CLIP (Contrastive Language–Image Pre-training) is a widely adopted vision–language model with a dual-tower architecture, consisting of an image encoder $F(\cdot)$ and a text encoder $G(\cdot)$. It is pre-trained using a large-scale set of image–text pairs through a contrastive learning objective that aligns visual and textual representations in a shared embedding space. Specifically, for each image–text pair (x, t) , CLIP maximizes the cosine similarity between the corresponding encoded features while minimizing similarities with mismatched pairs. This pre-training paradigm enables CLIP to acquire rich multimodal knowledge and strong zero-shot generalization capabilities across diverse downstream tasks.

Given a C -way classification problem with class names $\{t_c\}_{c=1}^C$, CLIP constructs textual features by feeding a hand-crafted prompt template (e.g., “*a photo of a* [CLASS]”) into the text encoder:

$$g_c = G(\text{prompt}(t_c)), \quad c = 1, \dots, C, \quad (1)$$

where $g_c \in \mathbb{R}^d$ denotes the textual feature of class c . For a test image x_i , the image encoder $F(\cdot)$ extracts its feature representation:

$$f_i = F(x_i). \quad (2)$$

where $f_i \in \mathbb{R}^d$. CLIP then computes the cosine similarity between f_i and each g_c , and applies a softmax operation to obtain the probability that x_i belongs to class c :

$$p_c(x_i) = \frac{\exp(\cos(f_i, g_c)/\tau)}{\sum_{j=1}^C \exp(\cos(f_i, g_j)/\tau)}, \quad (3)$$

where $\cos(\cdot)$ denotes the cosine similarity and τ is the temperature hyperparameter, typically set to 0.01. Benefiting from large-scale multimodal pretraining, CLIP exhibits excellent zero-shot recognition and strong cross-domain generalization.

3.2. Test-Time Padding (TTP)

As illustrated in Figure 3, we propose **Test-Time Padding (TTP)**, a lightweight test-time defense for CLIP that operates directly in the input space. Our approach is motivated by the key observation that applying padding to adversarial inputs partially restores disrupted attention, yielding a characteristic cosine-similarity shift between embed-

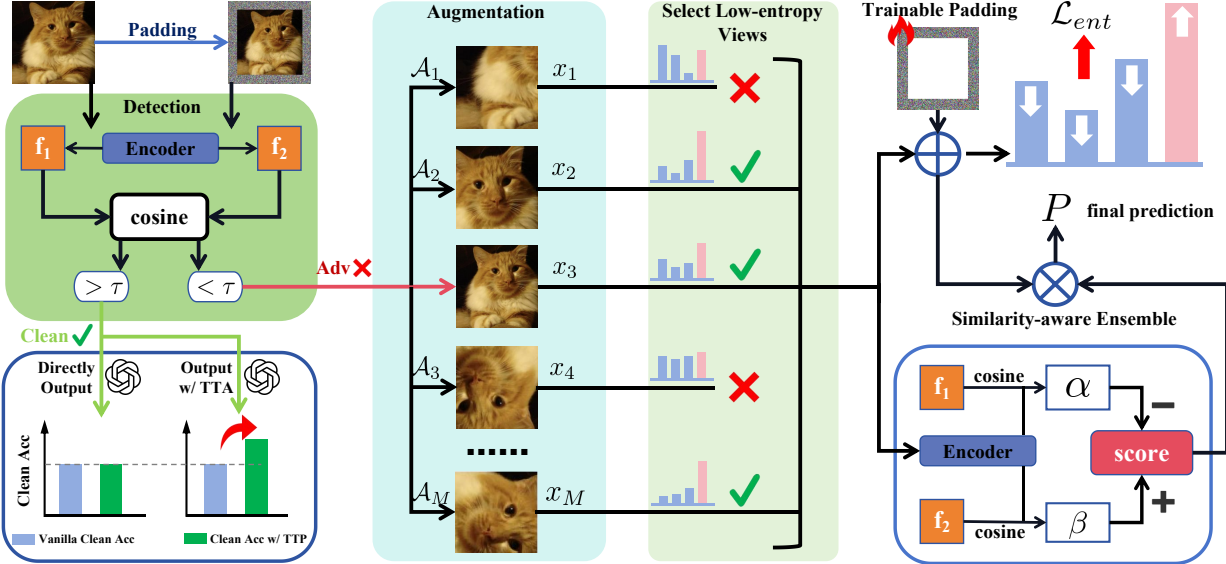


Figure 3. Overview of the proposed **Test-Time Padding (TPP)** pipeline. Given an input sample, CLIP image encoder features are extracted before and after applying padding. Their cosine similarity difference is compared with a universal threshold to distinguish clean versus adversarial inputs. Clean samples are directly recognized without adaptation. For adversarial examples, **trainable test-time padding** is activated to optimize padding parameters by entropy minimization using augmented views with low entropy. A **similarity-aware ensemble** then aggregates predictions across selected high-confidence views, ensuring a more reliable final prediction. Together, TPP enables accurate adversarial detection and adaptation-driven robustness improvement.

dings before and after padding. Clean samples exhibit minimal shift, whereas adversarial examples show pronounced change. This “similarity shift” provides a unified, model- and dataset-agnostic criterion for reliable detection without retraining.

Building on this, TPP forms a coherent three-stage pipeline: (1) we first perform **adversarial example detection** using the similarity shift to separate clean and adversarial inputs, allowing clean samples to bypass adaptation and thus preserving clean accuracy. (2) For detected adversarial examples, we employ **trainable test-time padding**, where instance-specific padding parameters are optimized by minimizing prediction entropy across confident augmented views, thereby better restoring the model’s attention. (3) Finally, a **similarity-aware ensemble** assigns distinct weights to each augmented view, leading to more robust predictions.

Adversarial example detection. Given a test sample x , we first apply a fixed padding operation $P^{\text{fix}}(x)$ and encode both x and $P^{\text{fix}}(x)$ using the frozen CLIP image encoder:

$$z = F(x), \quad z^{\text{pad}} = F(P^{\text{fix}}(x)). \quad (4)$$

The cosine similarity

$$s = \frac{z \cdot z^{\text{pad}}}{\|z\| \|z^{\text{pad}}\|} \quad (5)$$

is then compared against a threshold τ . If $s > \tau$, the sample is considered clean and is classified directly. Otherwise, it is treated as adversarial and passed on to the subsequent adaptive stages. This step addresses a critical limitation of prior test-time defense methods, which apply the same adaptation strategy to all inputs, by enabling sample-specific adaptation based on reliable detection. High detection accuracy also ensures that clean samples are largely unaffected, which preserves clean accuracy and enables the combination with other TTA methods to further improve performance.

Trainable test-time padding. For detected adversarial examples, following the widely adopted marginal entropy minimization paradigm in test-time adaptation [33, 35, 44], we generate multiple augmented views $\{x_i\}_{i=1}^N$ using stochastic transformations (e.g., random resize, crop, color jitter). Each view is encoded and classified to obtain prediction probabilities $p_c(x_i)$ and their Shannon entropies:

$$H_i = - \sum_{c=1}^C p_c(x_i) \log p_c(x_i). \quad (6)$$

The top-K low-entropy views form the confident subset B used for subsequent adaptation. Unlike prior test-time defenses that adapt textual prompt embeddings, our proposed method optimizes instance-specific image padding parameters at inference, for restoring clean attention patterns dis-

rupted by adversarial perturbations. More specifically, a lightweight trainable padding module $P_\theta(\cdot)$ is firstly applied to each augmented view x_i to obtain the corresponding augmented entropy H_i^{pad} . The parameter θ is then updated for a single step by minimizing the average entropy of the padded views:

$$\mathcal{L}_{\text{ent}} = \frac{1}{|B|} \sum_{i \in B} H_i^{\text{pad}}, \quad \theta \leftarrow \theta - \eta \nabla_\theta \mathcal{L}_{\text{ent}}. \quad (7)$$

Once updated, the padding module helps the model maintain stable predictions across multiple augmented adversarial views. Compared with random padding, this average entropy training strategy substantially reduces noise when restoring the model’s attention patterns.

Similarity-aware ensemble. After padding adaptation, we employ a similarity-based ensemble strategy, weighting the predictions from selected low-entropy views to obtain a more reliable final output. Specifically, for a given adversarial input x_{adv} , we first extract its image embedding before and after padding using the image encoder, yielding $z_{\text{adv}} = F(x_{\text{adv}})$ and $z_{\text{adv}}^{\text{pad}} = F(P_\theta(x_{\text{adv}}))$, respectively. For each selected augmented view x_i , we apply the trained padding module to obtain $P_\theta(x_i)$, then compute its image embedding $z_i^{\text{pad}} = F(P_\theta(x_i))$. Finally, the weight w_i assigned to each x_i is calculated as follows:

$$\alpha_i = \cos(z_i^{\text{pad}}, z_{\text{adv}}^{\text{pad}}), \quad (8)$$

$$\beta_i = \cos(z_i^{\text{pad}}, z_{\text{adv}}), \quad (9)$$

$$s_i = \alpha_i - \beta_i, \quad w_i = \frac{\exp(s_i)}{\sum_{j \in B} \exp(s_j)}. \quad (10)$$

Here, α_i is the cosine similarity between the padded embedding of x_i and the padded embedding of x_{adv} , while β_i measures similarity to the original adversarial embedding without padding. Because adversarial perturbations substantially distort image features, we prefer padded views that are farther from the original adversarial embedding (smaller β_i). However, simply increasing the distance from the adversarial example is not sufficient, as our objective is to achieve more accurate predictions. Our previous experiments demonstrate that trainable padding can effectively restore model attention, leading to highly similar attention maps with clean samples. Consequently, we also prefer augmented views closer to the padded adversarial embedding (larger α_i). Combining these insights, we use $s_i = \alpha_i - \beta_i$ as the view score and apply a softmax to obtain w_i , yielding a similarity-aware ensemble that prioritizes the most reliable views to maximize prediction accuracy. The final prediction is then computed as follows:

$$p_{\text{final}} = \arg \max_c \sum_{i \in B} w_i p_c(P_\theta(x_i)). \quad (11)$$

Algorithm 1: Test-Time Padding (TTP)

Input: Test sample x , frozen CLIP predictor $p_c(\cdot)$, detection threshold τ , number of augmented views N , fixed padding $P^{\text{fix}}(\cdot)$ and trainable padding $P_\theta(\cdot)$.

Output: Robust prediction p_{final}

Encode x and $P^{\text{fix}}(x)$ to measure similarity s (Eq. 5);

if $s > \tau$ **then**

return $p_c(x)$;

else

 Generate N augmented views $\{x_i\}_{i=1}^N$;

 Select low-entropy subset B ;

 Update $P_\theta(\cdot)$ by minimizing average entropy (Eq. 7);

 Compute weight w_i of each x_i (Eq. 10);

 Obtain final weighted prediction:

$p_{\text{final}} = \arg \max_c \sum_{i \in B} w_i p_c(P_\theta(x_i))$ (Eq. 11);

return p_{final} ;

By integrating adversarial detection, instance-specific padding adaptation, and similarity-aware ensemble, TTP provides a novel framework for test-time robustness enhancement. Operating entirely in the padding space, it requires neither text prompt tuning nor any model architectural knowledge or model modifications, making it a lightweight, efficient, and transferable defense mechanism. The total process of TTP is outlined in Algorithm 1.

4. Experiments

4.1. Setup

Datasets and Models. To evaluate the effectiveness of our test-time defense for vision-language models (VLMs), we conduct experiments on eight fine-grained classification datasets. These datasets cover a diverse range of domains, including general objects (Caltech101 [7]), animals (OxfordPets [30]), plants (Flower102 [29]), vehicles (Cars [17], Aircraft [25]), textures (DTD [4]), satellite imagery (EuroSAT [11]), and video-based actions (UCF101 [36]). Our experiments focus on CLIP as the backbone model, with three architectures considered: ViT-B/32, ViT-B/16 and ViT-L/14.

Evaluation and Baselines. To assess adversarial robustness, we follow the evaluation protocol of R-TPT [33], reporting accuracy on adversarial examples generated by PGD. We compare our method against two test-time defense baselines for CLIP: TTC [47] and the state-of-the-art method R-TPT [33], as well as two test-time adaptation baselines: Ensemble and MTA [49], and the zero-shot predictions from the original CLIP model. Here, Ensemble denotes simple averaging of predictions across all augmented views. All methods, including ours, use only the CLIP backbone and *AugMix* augmentation [12], without in-

Method	Caltech101		Pets		Cars		Flower102		Aircraft		DTD		EuroSAT		UCF101		Avg.	
	Acc.	Rob.																
CLIP [31]	91.4	0.2	85.1	0.0	60.1	0.0	64.0	0.0	18.1	0.0	43.0	0.0	35.8	0.0	61.6	0.0	57.4	0.0
TTC [47]	86.5	22.7	83.5	11.8	48.1	2.3	64.3	3.2	18.2	1.0	37.3	4.7	53.0	3.0	62.6	6.1	56.7	6.8
Ensemble	88.2	74.9	75.0	52.5	51.7	25.9	58.1	36.1	16.4	7.9	39.8	28.6	30.8	11.9	54.9	36.9	50.1	34.3
MTA [49]	92.0	76.3	86.3	53.6	63.4	26.4	64.4	36.5	20.2	8.2	43.8	28.8	34.6	11.3	63.3	39.1	58.3	35.0
R-TPT [33]	90.6	76.4	84.5	55.8	63.1	28.4	62.6	37.6	19.1	9.2	42.1	29.1	32.0	5.1	62.8	41.0	57.3	35.3
TTP (Ours)	90.9	81.8	84.7	61.0	59.8	29.8	63.6	42.0	18.0	10.3	42.8	32.2	35.6	14.1	61.3	46.6	57.1	39.7

Table 1. Clean (Acc.) and adversarial (Rob.) accuracy (%) on **fine-grained classification datasets** with pre-trained CLIP-ViT-B/32 ($\epsilon = 4.0$). The best results of clean accuracy are **bolded**, and the best results of robustness are **bolded**.

Method	Caltech101		Pets		Cars		Flower102		Aircraft		DTD		EuroSAT		UCF101		Avg.	
	Acc.	Rob.																
CLIP [31]	94.0	0.0	88.3	0.0	65.5	0.0	67.4	0.0	23.9	0.0	44.4	0.0	42.2	0.0	65.2	0.0	61.4	0.0
TTC [47]	87.6	8.4	82.3	10.4	55.0	2.9	69.0	7.4	23.3	0.5	41.0	4.5	47.4	0.4	65.8	1.6	58.9	4.5
Ensemble	91.9	74.7	86.2	51.2	65.7	26.0	65.9	36.3	23.4	8.7	43.2	25.1	28.2	2.2	63.0	30.6	58.4	31.8
MTA [49]	94.3	72.1	88.0	51.8	67.7	18.5	67.4	27.9	25.0	4.3	46.5	16.2	42.5	1.2	67.5	27.5	62.3	27.4
R-TPT [33]	93.7	82.0	87.2	60.2	67.0	34.7	68.7	44.6	23.9	13.2	46.4	32.8	34.7	8.5	67.2	43.2	61.1	39.9
TTP (Ours)	93.5	82.3	88.3	64.7	65.4	37.4	67.3	47.2	23.9	14.8	44.1	36.0	42.0	14.5	65.0	47.2	61.2	42.9

Table 2. Adversarial (Rob.) and Clean (Acc.) accuracy (%) on **fine-grained classification datasets** with pre-trained CLIP-ViT-B/16 ($\epsilon = 4.0$). The best results of clean accuracy are **bolded**, and the best results of robustness are **bolded**.

corporating additional foundation models (e.g., LLMs) or external knowledge.

Implementation Details. For adversarial evaluation, we employ the PGD attack with 100 iterations and a perturbation bound of $\epsilon = 4.0$. The trainable padding module uses a padding size of 32, and the adversarial detection threshold is set to 0.8. During test-time adaptation, the padding parameters are randomly initialized within $[0, 10]$ (corresponding to pixel values in $[0, 255]$) and optimized with a single update step. The learning rate for padding is set to 5, and the augmented batch size is 64. All experiments are implemented in PyTorch and conducted on NVIDIA RTX 3090 GPUs.

4.2. Results

Results on various datasets. We first evaluate TTP on fine-grained classification datasets. As shown in Table 1, with ViT-B/32 as the backbone, our proposed TTP achieves an average adversarial accuracy of 39.7% under 100-step PGD attacks with $\epsilon = 4/255$. Across all benchmark datasets and baselines (i.e., TTC [47], Ensemble, MTA [49], and R-TPT [33]), TTP consistently delivers superior adversarial robustness, demonstrating that trainable test-time padding significantly improves model resilience against adversarial perturbations. Compared to the state-of-the-art method R-TPT, TTP achieves an average performance improvement of 4.4%.

Notably, TTC, which also adopts a detection-then-defense strategy, exhibits poor robustness under such a strong attack, with an average adversarial accuracy of just 6.8%. This is mainly due to its low detection accuracy on

adversarial examples in high-strength attack scenarios. As illustrated earlier in Figure 2, TTC suffers from limited detection accuracy across different datasets and model architectures. If the detection step fails to differentiate clean samples from adversarial ones, adversarial examples may be misclassified as clean and evade robust adaptation, while clean samples might erroneously undergo robust adaptation, resulting in a loss of clean accuracy. In contrast, TTP achieves nearly 100% detection accuracy across diverse model architectures and datasets (also shown in Figure 2), greatly improving the targeting of subsequent robust adaptation and substantially enhancing adversarial robustness.

Results of different CLIP backbones. For experimental completeness, we next explore the transferability of TTP by applying it to other commonly used CLIP backbones, including CLIP-ViT-B/16 and CLIP-ViT-L/14. As shown in Table 2 and 3, TTP consistently enhances robustness across all benchmarks relative to baseline methods. This robustness gain is maintained even as the model scale increases significantly, indicating that TTP generalizes well to large-scale vision-language models. Such robustness scalability highlights the broad applicability of TTP and its potential to serve as a lightweight yet general defense paradigm for future vision-language systems. This strong generalization capability arises from our adaptation strategy, which operates directly in the input pixel space, independent of specific text prompts or model architectures, requires neither access to model details nor any model modification, thereby enabling a truly plug-and-play defense that demonstrates strong generalization capacity.

Method	Caltech101		Pets		Cars		Flower102		Aircraft		DTD		EuroSAT		UCF101		Avg.	
	Acc.	Rob.																
CLIP [31]	95.2	0.1	93.1	0.0	76.8	0.0	76.2	0.0	30.0	0.0	52.4	0.0	55.1	0.0	73.7	0.0	69.1	0.0
TTC [47]	88.7	7.7	92.2	7.6	67.8	2.2	76.5	7.5	31.7	0.5	49.7	6.2	64.1	0.2	75.0	2.2	68.2	4.3
Ensemble	94.9	83.6	93.4	63.5	76.3	40.5	75.0	48.6	31.7	12.7	51.3	31.3	38.7	11.1	71.7	48.3	66.6	42.5
MTA [49]	95.8	83.1	93.7	64.9	78.4	36.6	76.1	44.2	32.7	8.0	53.4	27.2	47.8	7.5	74.7	47.5	69.1	39.9
R-TPT [33]	95.7	88.2	93.7	72.9	77.2	49.1	76.2	55.6	31.7	17.2	54.0	38.0	44.3	20.4	74.3	55.6	68.4	49.6
TPP (Ours)	95.1	88.6	93.1	76.3	76.8	51.1	76.1	58.7	29.2	17.7	52.3	41.3	55.0	21.6	73.6	57.4	68.9	51.6

Table 3. Adversarial (Rob.) and Clean (Acc.) accuracy (%) on **fine-grained classification datasets** with pre-trained CLIP-ViT-L/14 ($\epsilon = 4.0$). The best results of clean accuracy are **bolded**, and the best results of robustness are **bolded**.

Method	Caltech101	Pets	Cars	Flower102	Aircraft	DTD	EuroSAT	UCF101	Avg.
TPP (0)	98.8	99.2	99.8	95.8	99.7	95.7	99.1	99.8	98.5
TPP (random)	97.5	98.9	97.6	96.9	92.3	90.7	94.9	95.5	95.8
TPP (255)	98.9	99.4	99.6	97.1	99.8	96.2	98.5	99.7	98.7

Table 4. Detection accuracy (%) of TPP using different padding patterns on **fine-grained classification datasets** with pre-trained CLIP-ViT-B/32 ($\epsilon = 4.0$). The best results are **(bolded)**.

Method	Flowers				DTD			
	CW	DF	FGSM	Avg.	CW	DF	FGSM	Avg.
CLIP [31]	0.8	0.4	4.8	2.0	2.3	7.6	13.4	7.8
R-TPT [33]	51.6	54.7	49.2	51.8	34.2	35.9	32.5	34.2
TPP (Ours)	54.1	56.4	51.8	54.1	38.9	40.1	37.1	38.7

Table 5. Adversarial accuracies (%) under CW, DeepFool (DF), and FGSM attacks on two fine-grained datasets. TPP achieves more robust performance. The best results of robustness are **bolded**.

Method	ViT-B/32	ViT-B/16	ViT-L/14	Avg.
CLIP [31]	57.4	61.4	69.1	62.6
TTC [47]	58.9	56.7	68.2	61.3
R-TPT [33]	57.1	61.1	68.4	62.2
TPP (Ours)	57.1	61.2	68.9	62.4
TPP (with TPT [35])	57.9	62.1	69.5	63.2

Table 6. Average clean accuracy (Acc.) of various test-time defenses across fine-grained classification datasets under various CLIP architectures. The best results of clean accuracy are **bolded**

Robustness under Various Attacks. To further examine the versatility and generalization of our method, we evaluate TPP and SOTA defense R-TPT under multiple adversarial attacks beyond PGD. Specifically, we employ CW [2], DeepFool [28], and FGSM [9] to assess robustness. The results on two fine-grained benchmarks are reported in Table 5. Across all types of attacks, TPP consistently achieves the highest adversarial accuracy, demonstrating stable and substantial gains over existing SOTA defense. These results confirm that TPP effectively mitigates a broad spectrum of adversarial attacks, establishing its versatility and attack-agnostic defense capability.

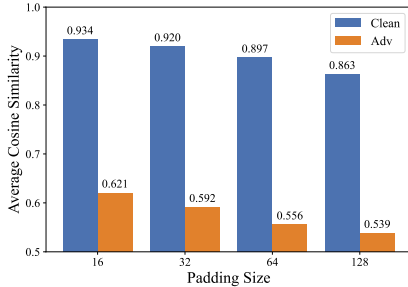
Integrate with test-time adaptation. In our proposed TPP, once an input is detected as clean, it bypasses ro-

bust adaptation and is directly forwarded for prediction. Because TPP achieves nearly 100% detection accuracy across diverse architectures and datasets, its clean accuracy closely matches that of vanilla CLIP, effectively preserving CLIP’s zero-shot generalization. Furthermore, benefiting from the detect-then-adapt strategy, samples classified as clean can be further enhanced using existing test-time adaptation methods. Taking the test-time adaptation baseline TPT [35] as an example, Table 6 shows that when combined with TPT, TPP achieves the highest clean accuracy among all test-time defenses. This accuracy could even be further improved by combining TPP with stronger test-time adaptation methods. It demonstrates that TPP can be seamlessly integrated with any existing test-time adaptation method, achieving SOTA results on both clean accuracy and adversarial robustness. These results highlight the flexibility and effectiveness of our approach.

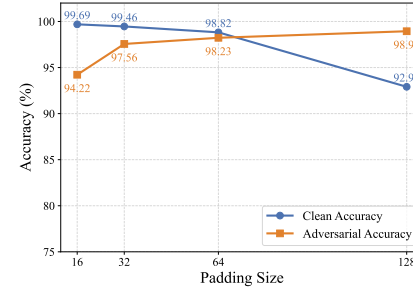
4.3. Ablation Study

Padding pattern for detection In TPP, we detect adversarial inputs using a fixed, training-free padding scheme. We therefore examine how different padding patterns affect detection accuracy. The results in Table 4 show that, with a predefined threshold ($\tau = 0.8$), TPP achieves consistently high accuracy on both clean and adversarial examples. Under random padding, overall detection accuracy reaches 95%, while 0 padding (all black) and 255 padding (all white) further raise it to 98.5% and 98.7%, respectively. These findings indicate that simpler padding patterns yield greater accuracy gains in the detection stage; accordingly, we can adopt 0 or 255 padding for better detection.

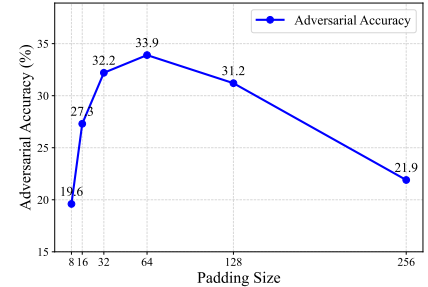
Padding Size. We conduct a systematic analysis of how padding size influences both adversarial detection accuracy and downstream robustness. For detection, we measure the cosine similarity between CLIP-encoded visual embed-



(a) Average cosine similarity.



(b) Detection accuracy.



(c) Adversarial Accuracy (Rob.) on DTD dataset.

Figure 4. Impact of padding size on adversarial detection and robust adaptation. ViT-B/32 is used as the CLIP backbone. The figure comprises three subplots: (a) average cosine similarities on fine-grained classification datasets of CLIP embeddings before and after padding across varying padding sizes, (b) detection accuracy for both adversarial and clean inputs, and (c) adversarial accuracy on the DTD dataset.

dings of clean samples and adversarial examples, computed before and after applying fixed zero-value spatial padding of varying sizes. A constant detection threshold of 0.8 is used for all settings. As shown in Figure 4a, increasing the padding size consistently reduces the cosine similarity for adversarial examples, while inducing only minor changes for clean samples. This widening gap between the two classes at moderate padding sizes directly improves detection accuracy by increasing separability in embedding space. However, when padding becomes excessively large, the gap begins to narrow—likely because extreme spatial alteration disrupts the original image layout, thereby degrading both clean and adversarial feature consistency.

For robustness, we further evaluate the effect of padding size on adversarial accuracy using the DTD dataset under PGD attack. Results in Figure 4c reveal a clear trend: performance initially rises with increasing padding size, reaching a peak at moderate values, before declining as padding grows larger. This pattern aligns with our attention-restoration hypothesis; moderate padding appears to sufficiently mitigate adversarial effects and recover attention without compromising structural integrity, whereas overly large padding corrupts spatial context and thus undermines the model’s ability to make reliable predictions. Taken together, these findings indicate that padding size must be carefully chosen to balance the benefits of attention restoration with the risks of structural distortion, with moderate padding emerging as the optimal setting for both high detection accuracy and strong adversarial robustness.

Components of TTP. We finally conduct ablation studies on all fine-grained classification datasets using ViT-B/32 and ViT-B/16 to evaluate the contribution of each component in our proposed TTP. As shown in Table 7, introducing fixed spatial padding already substantially enhances robustness by partially restoring model attention, validating the effectiveness of our padding strategy. To further improve attention recovery, we employ entropy minimization (Ent-

Sim-Aware	EntMin	Padding	ViT-B/32	ViT-B/16
✗	✗	✗	0.0	0.0
✗	✗	✓	37.5	38.0
✗	✓	✓	39.0	40.8
✓	✗	✓	38.3	39.5
✓	✓	✓	39.7	42.9

Table 7. **Ablation study of TTP components.** Adversarial accuracy (%) on **fine-grained classification datasets** using ViT-B/32 and ViT-B/16 backbones.

Min) to perform single-step training of the padding module during inference. Experimental results show that EntMin further boosts the model’s defensive performance. Finally, by integrating a similarity-aware ensemble, we apply additional weighting to low-entropy views for more reliable predictions. Table 7 demonstrates that TTP with all components achieves the best overall performance, confirming the indispensability of each module and reinforcing the effectiveness of our approach.

5. Conclusion

This work introduces Test-Time Padding (TTP), a lightweight and unified defense for CLIP that achieves robust inference without retraining or architectural modification. TTP hinges on a padding-induced embedding similarity shift that reliably separates clean from adversarial inputs across various datasets and backbones, followed by targeted, single-step trainable padding and a similarity-aware ensemble to restore disrupted attention and stabilize predictions. Extensive experiments on multiple CLIP variants and fine-grained benchmarks show that TTP consistently surpasses prior test-time defenses, delivering substantial robustness gains while preserving clean accuracy. Beyond its empirical strength, TTP offers a practical blueprint for test-

time defenses: detect first, then adapt, operating directly in the input space and remaining compatible with existing test-time adaptation techniques for optional clean-accuracy improvements.

References

- [1] Michael Ahn, Anthony Brohan, Noah Brown, Yevgen Chebotar, Omar Cortes, Byron David, Chelsea Finn, Chuyuan Fu, Keerthana Gopalakrishnan, Karol Hausman, et al. Do as i can, not as i say: Grounding language in robotic affordances. *arXiv preprint arXiv:2204.01691*, 2022. 1
- [2] Nicholas Carlini and David Wagner. Towards evaluating the robustness of neural networks. In *IEEE Symposium on Security and Privacy (SP)*, 2017. 7
- [3] Fei-Long Chen, Du-Zhen Zhang, Ming-Lun Han, Xiu-Yi Chen, Jing Shi, Shuang Xu, and Bo Xu. Vlp: A survey on vision-language pre-training. *Machine Intelligence Research*, 20(1):38–56, 2023. 1
- [4] Mircea Cimpoi, Subhransu Maji, Iasonas Kokkinos, Sammy Mohamed, and Andrea Vedaldi. Describing textures in the wild. In *CVPR*, pages 3606–3613, 2014. 5
- [5] Hao Fang, Jiawei Kong, Bin Chen, Tao Dai, Hao Wu, and Shu-Tao Xia. Clip-guided generative networks for transferable targeted adversarial attacks. In *ECCV*, pages 1–19. Springer, 2024. 1
- [6] Hao Fang, Jiawei Kong, Wenbo Yu, Bin Chen, Jiawei Li, Hao Wu, Shutao Xia, and Ke Xu. One perturbation is enough: On generating universal adversarial perturbations against vision-language pre-training models. *arXiv preprint arXiv:2406.05491*, 2024. 3
- [7] Li Fei-Fei, Rob Fergus, and Pietro Perona. Learning generative visual models from few training examples: An incremental bayesian approach tested on 101 object categories. In *CVPRW*, pages 178–178, 2004. 5
- [8] Chun-Mei Feng, Kai Yu, Yong Liu, Salman Khan, and Wangmeng Zuo. Diverse data augmentation with diffusions for effective test-time prompt tuning. In *ICCV*, pages 2704–2714, 2023. 3
- [9] Ian J Goodfellow, Jonathon Shlens, and Christian Szegedy. Explaining and harnessing adversarial examples. *arXiv preprint arXiv:1412.6572*, 2014. 2, 3, 7
- [10] Bangyan He, Xiaojun Jia, Siyuan Liang, Tianrui Lou, Yang Liu, and Xiaochun Cao. Sa-attack: Improving adversarial transferability of vision-language pre-training models via self-augmentation. *arXiv preprint arXiv:2312.04913*, 2023. 3
- [11] Patrick Helber, Benjamin Bischke, Andreas Dengel, and Damian Borth. Eurosat: A novel dataset and deep learning benchmark for land use and land cover classification. *IEEE Journal of Selected Topics in Applied Earth Observations and Remote Sensing*, 12(7):2217–2226, 2019. 5
- [12] Dan Hendrycks, Norman Mu, Ekin D Cubuk, Barret Zoph, Justin Gilmer, and Balaji Lakshminarayanan. Augmix: A simple data processing method to improve robustness and uncertainty. *arXiv preprint arXiv:1912.02781*, 2019. 5
- [13] Zhi Huang, Federico Bianchi, Mert Yuksekogul, Thomas J Montine, and James Zou. A visual–language foundation model for pathology image analysis using medical twitter. *Nature Medicine*, 29(9):2307–2316, 2023. 1
- [14] Chao Jia, Yinfei Yang, Ye Xia, Yi-Ting Chen, Zarana Parekh, Hieu Pham, Quoc Le, Yun-Hsuan Sung, Zhen Li, and Tom Duerig. Scaling up visual and vision-language representation learning with noisy text supervision. In *International Conference on Machine Learning*, pages 4904–4916. PMLR, 2021. 1
- [15] Adilbek Karmanov, Dayan Guan, Shijian Lu, Abdulmotaleb El Saddik, and Eric Xing. Efficient test-time adaptation of vision-language models. In *CVPR*, pages 14162–14171, 2024. 3
- [16] Dehong Kong, Siyuan Liang, Xiaopeng Zhu, Yuansheng Zhong, and Wenqi Ren. Patch is enough: naturalistic adversarial patch against vision-language pre-training models. *Visual Intelligence*, 2(1):1–10, 2024. 1
- [17] Jonathan Krause, Michael Stark, Jia Deng, and Li Fei-Fei. 3d object representations for fine-grained categorization. In *IEEE International Conference on Computer Vision Workshops*, pages 554–561, 2013. 5
- [18] Alexey Kurakin, Ian J Goodfellow, and Samy Bengio. Adversarial examples in the physical world. In *Artificial intelligence safety and security*, pages 99–112. Chapman and Hall/CRC, 2018. 3
- [19] Lin Li, Haoyan Guan, Jianing Qiu, and Michael Spratling. One prompt word is enough to boost adversarial robustness for pre-trained vision-language models. In *CVPR*, 2024. 1, 3
- [20] Jian Liang, Ran He, and Tieniu Tan. A comprehensive survey on test-time adaptation under distribution shifts. *IJCV*, 133(1):31–64, 2025. 3
- [21] Dong Lu, Zhiqiang Wang, Teng Wang, Weili Guan, Hongchang Gao, and Feng Zheng. Set-level guidance attack: Boosting adversarial transferability of vision-language pre-training models. In *ICCV*, pages 102–111, 2023. 3
- [22] Xiaosong Ma, Jie Zhang, Song Guo, and Wenchao Xu. Swapprompt: Test-time prompt adaptation for vision-language models. In *NeurIPS*, pages 65252–65264, 2023. 3
- [23] Xingjun Ma, Linxi Jiang, Hanxun Huang, Zejia Weng, James Bailey, and Yu-Gang Jiang. Imbalanced gradients: a subtle cause of overestimated adversarial robustness. *Machine Learning*, 113(5):2301–2326, 2024. 3
- [24] Aleksander Madry, Aleksandar Makelov, Ludwig Schmidt, Dimitris Tsipras, and Adrian Vladu. Towards deep learning models resistant to adversarial attacks. *arXiv preprint arXiv:1706.06083*, 2017. 2, 3
- [25] Subhransu Maji, Esa Rahtu, Juho Kannala, Matthew Blaschko, and Andrea Vedaldi. Fine-grained visual classification of aircraft. *arXiv preprint arXiv:1306.5151*, 2013. 5
- [26] Chengzhi Mao, Scott Geng, Junfeng Yang, Xin Wang, and Carl Vondrick. Understanding zero-shot adversarial robustness for large-scale models. In *ICLR*, 2023. 1, 3
- [27] Fan'an Meng, Chaoran Cui, Hongjun Dai, and Shuai Gong. Black-box test-time prompt tuning for vision-language models. In *AAAI*, pages 6099–6107, 2025. 3

- [28] Seyed-Mohsen Moosavi-Dezfooli, Alhussein Fawzi, and Pascal Frossard. Deepfool: a simple and accurate method to fool deep neural networks. In *CVPR*, pages 2574–2582, 2016. 7
- [29] Maria-Elena Nilsback and Andrew Zisserman. Automated flower classification over a large number of classes. In *Sixth Indian Conference on Computer Vision, Graphics & Image Processing*, pages 722–729. IEEE, 2008. 5
- [30] Omkar M Parkhi, Andrea Vedaldi, Andrew Zisserman, and CV Jawahar. Cats and dogs. In *CVPR*, pages 3498–3505, 2012. 5
- [31] Alec Radford, Jong Wook Kim, Chris Hallacy, Aditya Ramesh, Gabriel Goh, Sandhini Agarwal, Girish Sastry, Amanda Askell, Pamela Mishkin, Jack Clark, et al. Learning transferable visual models from natural language supervision. In *International Conference on Machine Learning*, 2021. 1, 6, 7
- [32] Jameel Abdul Samad, Mohammad Hanan Gani, Noor Husseini, Muhammad Uzair Khattak, Muhammad Muzammal Naseer, Fahad Shahbaz Khan, and Salman H Khan. Align your prompts: Test-time prompting with distribution alignment for zero-shot generalization. In *NeurIPS*, pages 80396–80413, 2023. 3
- [33] Lijun Sheng, Jian Liang, Zilei Wang, and Ran He. R-ptp: Improving adversarial robustness of vision-language models through test-time prompt tuning. In *CVPR*, pages 29958–29967, 2025. 2, 3, 4, 5, 6, 7, 1
- [34] Mohit Shridhar, Lucas Manuelli, and Dieter Fox. Cliprot: What and where pathways for robotic manipulation. In *Conference on Robot Learning*, pages 894–906. PMLR, 2022. 1
- [35] Manli Shu, Weili Nie, De-An Huang, Zhiding Yu, Tom Goldstein, Anima Anandkumar, and Chaowei Xiao. Test-time prompt tuning for zero-shot generalization in vision-language models. In *NeurIPS*, pages 14274–14289, 2022. 3, 4, 7
- [36] Khurram Soomro, Amir Roshan Zamir, and Mubarak Shah. A dataset of 101 human action classes from videos in the wild. *Center for Research in Computer Vision*, 2(11):1–7, 2012. 5
- [37] Elaine Sui, Xiaohan Wang, and Serena Yeung-Levy. Just shift it: Test-time prototype shifting for zero-shot generalization with vision-language models. In *IEEE/CVF Winter Conference on Applications of Computer Vision (WACV)*, pages 825–835. IEEE, 2025. 3
- [38] Christian Szegedy, Wojciech Zaremba, Ilya Sutskever, Joan Bruna, Dumitru Erhan, Ian Goodfellow, and Rob Fergus. Intriguing properties of neural networks. *arXiv preprint arXiv:1312.6199*, 2013. 1
- [39] Christian Szegedy, Wojciech Zaremba, Ilya Sutskever, Joan Bruna, Dumitru Erhan, Ian Goodfellow, and Rob Fergus. Intriguing properties of neural networks. In *ICLR*, 2014. 2
- [40] Baoshun Tong, Hanjiang Lai, Yan Pan, and Jian Yin. On the zero-shot adversarial robustness of vision-language models: A truly zero-shot and training-free approach. In *CVPR*, pages 19921–19930, 2025. 2
- [41] Dequan Wang, Evan Shelhamer, Shaoteng Liu, Bruno Olshausen, and Trevor Darrell. Tent: Fully test-time adaptation by entropy minimization. In *ICLR*, 2021. 3
- [42] Haodi Wang, Kai Dong, Zhilei Zhu, Haotong Qin, Aishan Liu, Xiaolin Fang, Jiakai Wang, and Xianglong Liu. Transferable multimodal attack on vision-language pre-training models. In *IEEE Symposium on Security and Privacy (SP)*, pages 1722–1740. IEEE, 2024. 3
- [43] Xin Wang, Kai Chen, Xingjun Ma, Zheneng Chen, Jingjing Chen, and Yu-Gang Jiang. Advqdet: Detecting query-based adversarial attacks with adversarial contrastive prompt tuning. In *ACM MM*, pages 6212–6221, 2024. 1
- [44] Xin Wang, Kai Chen, Jiaming Zhang, Jingjing Chen, and Xingjun Ma. Tapt: Test-time adversarial prompt tuning for robust inference in vision-language models. In *CVPR*, pages 19910–19920, 2025. 2, 3, 4
- [45] Zifeng Wang, Zhenbang Wu, Dinesh Agarwal, and Jimeng Sun. Medclip: Contrastive learning from unpaired medical images and text. In *Conference on Empirical Methods in Natural Language Processing*, page 3876, 2022. 1
- [46] Dongxian Wu, Shu-Tao Xia, and Yisen Wang. Adversarial weight perturbation helps robust generalization. In *NeurIPS*, pages 2958–2969, 2020. 3
- [47] Songlong Xing, Zhengyu Zhao, and Nicu Sebe. Clip is strong enough to fight back: Test-time counterattacks towards zero-shot adversarial robustness of clip. In *CVPR*, pages 15172–15182, 2025. 2, 3, 5, 6, 7, 1
- [48] Yongcan Yu, Lijun Sheng, Ran He, and Jian Liang. Benchmarking test-time adaptation against distribution shifts in image classification. *arXiv preprint arXiv:2307.03133*, 2023. 3
- [49] Maxime Zanella and Ismail Ben Ayed. On the test-time zero-shot generalization of vision-language models: Do we really need prompt learning? In *CVPR*, pages 23783–23793, 2024. 3, 5, 6, 7, 1
- [50] Hongyang Zhang, Yaodong Yu, Jiantao Jiao, Eric Xing, Laurent El Ghaoui, and Michael Jordan. Theoretically principled trade-off between robustness and accuracy. In *International Conference on Machine Learning*, pages 7472–7482. PMLR, 2019. 3
- [51] Jiaming Zhang, Qi Yi, and Jitao Sang. Towards adversarial attack on vision-language pre-training models. In *ACM MM*, pages 5005–5013, 2022. 3
- [52] Jingyi Zhang, Jiaxing Huang, Sheng Jin, and Shijian Lu. Vision-language models for vision tasks: A survey. *IEEE TPAMI*, 2024. 1
- [53] Peng-Fei Zhang, Zi Huang, and Guangdong Bai. Universal adversarial perturbations for vision-language pre-trained models. In *47th International ACM SIGIR Conference on Research and Development in Information Retrieval*, pages 862–871, 2024. 3
- [54] Yunqing Zhao, Tianyu Pang, Chao Du, Xiao Yang, Chongxuan Li, Ngai-Man Cheung, and Min Lin. On evaluating adversarial robustness of large vision-language models. In *NeurIPS*, pages 54111–54138, 2023. 1
- [55] Yiwei Zhou, Xiaobo Xia, Zhiwei Lin, Bo Han, and Tongliang Liu. Few-shot adversarial prompt learning on vision-language models. In *NeurIPS*, pages 3122–3156, 2024. 1

- [56] Ziqi Zhou, Shengshan Hu, Minghui Li, Hangtao Zhang, Yechao Zhang, and Hai Jin. Advclip: Downstream-agnostic adversarial examples in multimodal contrastive learning. In *ACM MM*, pages 6311–6320, 2023. 3

TPP: Test-Time Padding for Adversarial Detection and Robust Adaptation on Vision-Language Models

Supplementary Material

A. Overview

This supplementary material presents comprehensive dataset details and additional experiments that were omitted from the main paper due to space constraints. These results further substantiate the effectiveness of our proposed Test-Time Padding (TPP).

B. Datasets

We summarize the content, number of categories and number of images for all datasets used in our experiments in Table 8.

Dataset	Description	# Classes	# Test
Caltech101	Object images	100	2,465
Pets	Pet images	37	3,669
Cars	Car images	196	8,041
Flower102	Flower images	102	2,463
Aircraft	Aircraft images	100	3,333
DTD	Describable textures dataset	47	1,692
EuroSAT	Sentinel-2 satellite images	10	8,100
UCF101	Human action images	101	3,783

Table 8. All datasets involved in our experiments.

C. Results of Different Thresholds

As demonstrated in Figure 4a of the main paper, with a padding size of 32, clean samples and adversarial examples exhibit significant differences in average cosine similarity when compared to their padded versions. Consequently, a preset threshold τ can be effectively employed to distinguish between them. In our experiments, we empirically set $\tau = 0.8$, which yielded robust cross-dataset and cross-model detection performance (as shown in Figure 2).

To ensure experimental integrity, we further investigated the sensitivity of detection accuracy to variations in the threshold value. As illustrated in Figure 5, our method consistently achieves optimal performance at $\tau = 0.8$ across all datasets. This indicates that our approach is dataset-agnostic, allowing for the use of a unified hyperparameter τ without the burden of extensive tuning, thereby underscoring the practical utility of TPP. Furthermore, detection accuracy degrades when the threshold deviates (either lower or higher) from this optimal value. This behavior is consistent with the cosine similarity distributions between clean samples and adversarial examples before and after padding, as illustrated in Figure 4a.

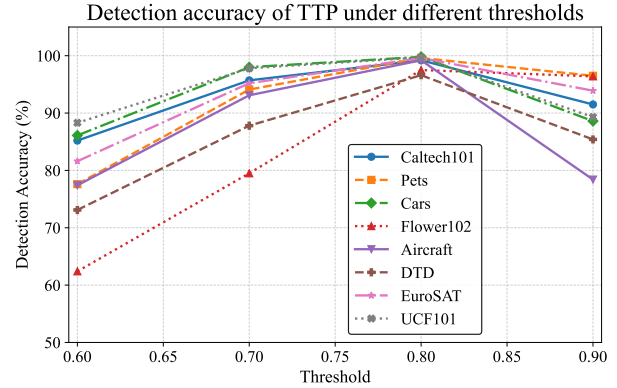


Figure 5. Detection accuracy of TPP with CLIP-ViT-B/32 ($\epsilon = 4.0$) under varying threshold values.

D. Robustness under Various Attacks

Due to space limitations in Section 4.2 of the main text, we restricted our comparison to the SOTA defense, R-TPT, under multiple adversarial attacks beyond PGD. To provide a comprehensive evaluation, we present a comparison against all baselines in this section. The results demonstrate that our proposed TPP consistently outperforms all competing baselines across the various attack scenarios.

Method	Flowers				DTD			
	CW	DF	FGSM	Avg.	CW	DF	FGSM	Avg.
CLIP [31]	0.8	0.4	4.8	2.0	2.3	7.6	13.4	7.8
TTC [47]	3.6	56.5	2.1	20.7	4.3	31.1	1.4	12.3
Ensemble	50.1	52.2	46.6	49.7	31.1	32.9	29.7	31.2
MTA [49]	34.5	35.4	36.6	35.5	23.6	23.5	23.9	23.7
R-TPT [33]	51.6	54.7	49.2	51.8	34.2	35.9	32.5	34.2
TPP (Ours)	54.1	56.4	51.8	54.1	38.9	40.1	37.1	38.7

Table 9. Adversarial accuracies (%) under CW, DeepFool (DF), and FGSM attacks on two fine-grained datasets. TPP achieves the best robustness across all attacks.